(N,V,T) Monte Carlo Simulations of the Electrostatic Interaction between Charged Colloids: Finite Size Effects

A. Delville

CRMD, CNRS, 1B rue de la Férollerie, 45071 Orléans Cedex 02, France

Received: March 17, 1999; In Final Form: July 27, 1999

We performed (N,V,T) Monte Carlo simulations of the ion distribution between two charged disks immersed in a large simulation cell. Ion−ion, ion−disk and disk−disk interactions are described in the framework of the primitive model. The purpose of these Monte Carlo simulations is to quantify the influence of interionic correlation forces on the stability of charged colloids. The net electrostatic and contact forces between the disks are calculated as a function of the counterion charge. While the same qualitative results were obtained for infinite charged lamellae, the finite size of the colloids has a strong influence on the different contributions to the net interparticle force. We also discuss the validity of the so-called Weak Overlap Approximation, which may be used to describe the interparticle force in a simplified treatment of colloidal suspensions based on the One Component Plasma approach.

1. Introduction

Charged colloids include a large class of biological (DNA, membranes, biopolymers), mineral (clays, metallic oxides), and synthetic (latex, cement, polyelectrolytes) particles. The understanding and prediction of their physicochemical properties (adsorption, ionic condensation, swelling or cohesive behavior, gelation) require a detailed description of their mutual interactions.

For that purpose, numerous numerical calculations and simulations have been performed in the framework of the primitive model[1−25] in order to describe the ionic clouds surrounding each charged particle. Many calculations were performed by using simple geometries (sphere,[2,4,10−12,15,17,19,24] infinite cylinder,[1] or plate[3,8−9,13,21−23]). These studies were further simplified by treating a single colloid immersed in a large volume.[4,7] While this approach is only valid for analyzing highly diluted suspensions, finite concentration effects were introduced by assuming perfect alignment of isolated cells centered on a single colloid and neglecting any direct intercolloidal interactions.[1,13]

Furthermore, many previous studies used the Poisson−Boltzmann approximation[1,4,7,16−18,20] in order to describe the ionic diffuse layers, while this approach neglects interionic correlations.[8−10,14,21−24] In that context, two different limiting conditions are useful,[25] assuming either a constant electric charge or potential at the surface of colloidal particles. While the last condition is valid only for describing metallic particles, the former condition is more appropriate for describing dielectric particles in the absence of ion-determining potential.[25] That condition corresponds to a large variety of colloids, including clays and polyelectrolytes resulting from the polymerization of strong acids (such as phosphate, sulfonate, acrylate, ...). The present Monte Carlo study is devoted to such dielectric colloids, while ion binding will be considered in a following study.

Recent Monte Carlo simulations[9,10,14,21−24] have determined the influence of interionic correlations forces by a direct calculation of interparticular forces from equilibrium configurations of the confined counterions. By contrast with the monotonic repulsion predicted in all cases by the Poisson−Boltzmann approach, these numerical simulations showed a large variety of attracto-repulsive behavior due to electrostatic and contact forces. Despite of the simplicity of the primitive model, nonmonotonic equation of state and phase coexistence may appear,[21] due to the occurrence of three antagonistic contributions:[21] entropic repulsion, electrostatic attraction and hard core repulsion. For infinite charged lamellae, the transition between these different attracto-repulsive regimes is monitored by the strength of the counterion/lamella electrostatic coupling[21−23]

$$\xi = \frac{\sigma_p z_i e a_i}{4\pi \epsilon_0 \epsilon_r kT}$$

where σ_p is the lamella surface charge density, $z_i e$ the electric charge of the counterion, ϵ_r the dielectric constant of the solvent, and a_i the ionic radius, i.e., the minimum ion/lamella separation. Under weak coupling conditions ($\xi \sim 0.1$ such as for sodium Montmorillonite dispersed in water, a case corresponding to $\sigma_p \sim 710^{-3}$ e/Å^2, $\epsilon_r = 80$, $z_i = 1$, and $a_i = 2.25$ Å), ionic correlations are negligible, and monotonic swelling is observed resulting from entropic repulsion due to the overlap of the ionic diffuse layers of counterions confined between the two lamellae. At larger coupling ($\xi \sim 0.2$, i.e. for calcium Montmorillonite), cohesion is detected due to attractive electrostatic correlation forces. Finally, under extreme coupling conditions ($\xi \geq 0.5$, i.e. for cement particles, a case corresponding to $\sigma_p \geq 3 \times 10^{-2}$ e/Å^2, $\epsilon_r = 80$, $z = 2$, and $a_i = 2.5$ Å) strong repulsion occurs as a result of interionic excluded volume effects.

One may ask about the validity of such predictions obtained under idealized conditions, i.e., for infinite uniformly charged lamellae. Recent simulations have thus been performed to determine the influence of the size of charged spherical colloids on their mutual interaction.[15,24] However, the mechanical behavior of charged discotic particles has not yet been investigated, despite the great interest manifested recently for such self-ordering systems.[26−31] Preliminary simulations confirm the influence of both electrostatic[31,32] and entropic[31,33] effects on

10.1021/jp990938i CCC: $18.00
Published on Web 09/10/1999

the structural, mechanical, and dynamical properties of diluted suspensions of such discotic charged colloids.

We have thus performed (N,V,T) Monte Carlo simulations of the distribution of neutralizing sodium and calcium counterions between two parallel charged hard disks immersed in a large simulation cell. The origin of the net interparticle force between such finite colloids differs totally from that of infinite lamellae. However, we obtain the same qualitative mechanical behavior, i.e., repulsion or attraction as a function of the coupling parameter.[22−23]

2. Methods

We performed (N,V,T) Monte Carlo simulations of the distribution of 842 monovalent and 421 divalent counterions neutralizing two parallel negatively charged disks. The ion/ion, disk/ion and disk/disk interactions are described in the framework of the primitive model: electrostatic long-ranged coupling and hard core contact repulsion. Ion diameter ($2a_i$) is set to 4.5 Å for both counterions, corresponding to the size of hydrated sodium and calcium cations.

The diameter and thickness of charged disks were set to 200 and 5.5 Å, respectively, to model the behavior of synthetic Laponite clay.[31] These clay particles result from the sandwiching of one layer of octahedral magnesium oxide between two layers of tetrahedral silicium oxide. The electric charge of the Laponite particle originates from substitution of some Mg^{2+} cations of the octahedral network by Li^+ cations, leading to negative charges neutralized by interlamellar cations. To mimic the behavior of these clays, 421 negative charges are displayed on a squared lattice located within the equatorial plane of each disk. The corresponding surface charge density is 0.0067 electron per squared Å of total basal surface.

Because of the amphoteric nature of the lateral sites, positive and negative charges occur as a function of the pH of the suspension. These charges are neglected in the present study, since our experiments on Laponite suspensions[27,31,37] were performed at pH $\sim$ 10 in order to prevent the appearance of lateral charges, because they lead also to dissolution of this synthetic clay.[38] In any case, positive or negative lateral charges may be included in Monte Carlo studies of interparticular forces. As previously stated, positive lateral charges are expected to promote edge/basal surface attraction, leading to the so-called "house-cards" structure.[39]

Calculations are performed for fixed relative geometries: the two charged disks remain parallel to each other, at constant center/center separation. For symmetry reasons, the average torque acting on each particle is equal to zero. The separation between the particles (D) is renormalized through reference to the ionic diameter ($D^* = D/(2a_i)$).

In addition to the electrostatic energy, we also determined the average force acting on each particle in the longitudinal direction (along the $\mathbf{e}_z$ director). This force divided by the cross section of the particle may be directly compared with the pressure determined for infinite particles. It originates from the ion/particle and particle/particle electrostatic and contact forces. The electrostatic energy is calculated using Ewald summation,[34] within the classical 3D minimum image convention:

$$E_{el} = E_{dir} + E_{self} + E_{mom} + E_{rec} \tag{1a}$$

$$E_{dir} = \frac{0.5}{4\pi\epsilon_0\epsilon_r}\sum_i q_i \sum_{j\neq i}\frac{q_j\, erfc(\kappa r_{ij})}{r_{ij}} \tag{1b}$$

$$E_{self} = -\frac{\kappa}{\sqrt{\pi}4\pi\epsilon_0\epsilon_r}\sum_i {q_i}^2 \tag{1c}$$

$$E_{mom} = \frac{2\pi}{V(1+2\epsilon_\infty)4\pi\epsilon_0\epsilon_r}\Big(\sum_i q_i\,\mathbf{r}_i\Big)^2 \tag{1d}$$

$$E_{rec} = \frac{2\pi}{V4\pi\epsilon_0\epsilon_r}\sum_{K\neq 0}\frac{\exp(-K^2/4\kappa^2)}{K^2}\Big[\Big\{\sum_i q_i\cos(\mathbf{K}\mathbf{r}_i)\Big\}^2 + \Big\{\sum_i q_i\sin(\mathbf{K}\mathbf{r}_i)\Big\}^2\Big] \tag{1e}$$

where e_∞, the dielectric constant of the continuum surrounding the replica of the central simulation cell, is set equal to 1.

The longitudinal component of the force acting on a particle p is obtained by derivation of eqs 1

$$\mathbf{F}_{zdir} = \sum_{i\in p} q_i \sum_{j\notin p} q_j \left[\frac{2\kappa r_{ij}\exp(-\kappa^2 {r_{ij}}^2) + \sqrt{\pi}\, erfc(\kappa r_{ij})}{\sqrt{\pi}\,4\pi\epsilon_0\epsilon_r}\right]\frac{\mathbf{r}_{zij}}{{r_{ij}}^3} \tag{2a}$$

$$\mathbf{F}_{zrec} = -\frac{1}{\epsilon_0\epsilon_r V}\sum_{i\in p} q_i \sum_{\mathbf{K}\neq\mathbf{0}}\frac{\mathbf{K}_z\exp(-K^2/4\kappa^2)}{K^2}\sum_{j\notin p} q_j\sin(\mathbf{K}\mathbf{r}_{ij}) \tag{2b}$$

plus the ion/contact contribution

$$\mathbf{F}_{zcont} = kT\int_{surf} c_i(0)\,\mathbf{n}_z\,ds \tag{2c}$$

where $c_i(0)$ is the counterion density at contact with the basal surfaces of the disk, $\mathbf{e}_z$ the longitudinal director, and $\mathbf{n}_z$ the normal to the disk surface.

Summations in the reciprocal space (eqs 1e and 2b) are performed with 728 replica of the central cell, and the screening parameter κ is set to 0.005 $Å^{-1}$. Since the size of the simulation cell is 1000 Å, these conditions lead to an accuracy better than 0.005 for the electrostatic energy.[40] Longitudinal contact forces exerted on each particle are determined by extrapolating to contact the local ionic densities on both sides of the disk. To reduce the statistical noise, 5000 blocks of 20 000 iterations were necessary to thermalize and average the interparticle force.

Monte Carlo simulations of the interaction between two infinite charged lamellae were performed as previously, by using an external self-consistent field,[3,5,9] to reproduce the long range of the electrostatic potential cut by the 2D minimum image convention. This procedure was shown to be equivalent to 2D Ewald summation[35] and was comparable to an analytic treatment of the electrostatic interactions within such a heterogeneous system performed by using hyperspherical geometry.[21−22]

3. Results and Discussion

(A) Ionic Distribution. Figure 1 shows a snapshot of equilibrium configuration of 427 divalent counterions distributed around two charged disks with a center to center separation of 22 Å. Because of the finite thickness of the disks (5.5 Å, see Section 2), this separation corresponds to an available interparticular space (D) of 76.5 Å or 3.67 reduced units ($D^* = D/(2a_i)$). The distribution of neutralizing counterions between two infinite lamellae was the subject of numerous studies[3,5,8−9,13,14,21−23] since it determines their mutual interaction

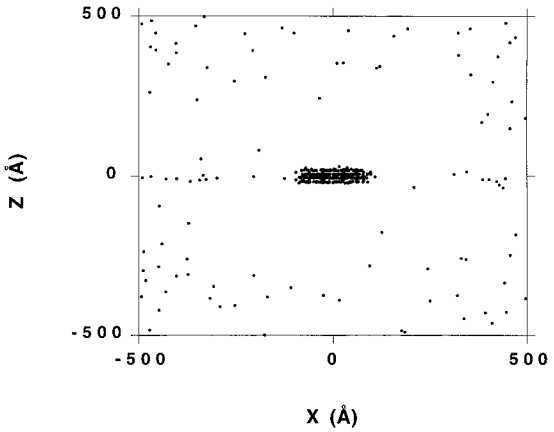

Figure 1. Lateral projection in the (*X*,*Z*) plane of a snapshot of the distribution of 421 divalent counterions around two parallel charged disks with a center/center separation of 22 Å ($D^* = 3.67$). The width of the figure is 1000 Å, and the origin is set at the center of the cell. The two parallel colloids are easily visualized by their cloud of condensed counterions.

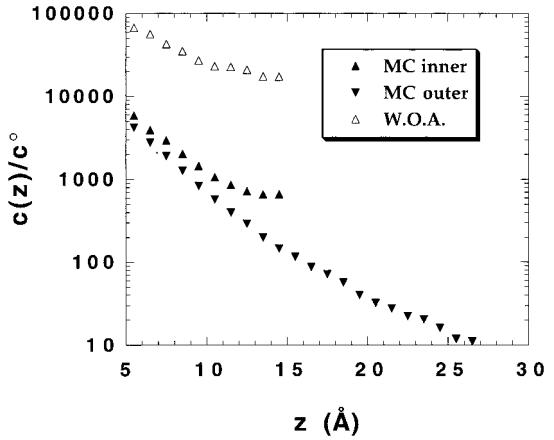

Figure 2. Local ionic concentration profiles (in reduced units [$c_i(z)/c_i^\circ$]) of monovalent counterions condensed in the inner and outer domains around each charged disk for a center/center separation of 30 Å (see text). The local concentrations of condensed counterions are averaged within a cylindrical shell (diameter 200 Å) located at a longitudinal separation *z* from the center of the nearest disk.

by screening the particle/particle electrostatic repulsion. However, for finite particles, the behavior of the system is more complex since the neutralizing counterions are not necessarily confined between the particles.[16,18,20,26−31]

Average concentration profiles are drawn in Figure 2 for ions located in a cylinder limited by the cross section of the disks. Since the origin is set at the center of each disk, the densities of counterions at contact with the basal surfaces of the disks are obtained by extrapolating the concentration profiles down to a distance of 5 Å (i.e., one-half of the particle thickness plus the ionic radius). Figure 2 exhibits noticeable differences between the local ionic concentrations inside and outside the interparticular domains. The ionic densities are always larger in the interparticular domain because of the overlap of the electrostatic well located in the vicinity of each particle which leads to ionic condensation. This overlap is important since the net contact force acting on each particle results from a balance between its inner and outer ionic contact densities (cf. eq 2c).

Another consequence of the dissymmetry of the ionic concentration profiles concerns the mean force potential

$$W_i(r) = -kT \log(c_i(r)/c_i^\circ) \qquad (3)$$

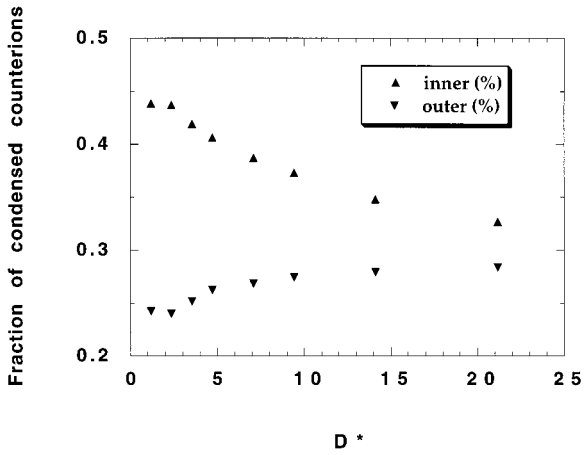

Figure 3. Fraction of inner and outer (see text) condensed monovalent counterions obtained from integration of Figure 2.

where c_i° is the average ionic concentration in the simulation cell. Since the mean force potential differs on both side of the particle, one cannot describe ionic distribution between such dielectric particles by solving the Poisson−Boltzmann equation using the same limiting surface potential on both sides of the charged lamellae.[25,36] Such an approach is only valid for metallic particles, for which the Dirichlet limiting conditions on the electrostatic potential are valid at the lamella surface.

One may be tempted to use the Weak Overlap Approximation in order to describe the interaction between a large collection of charged particles in the framework of the One Component Plasma. As shown in Figure 2, this simple additivity rule overestimates the local concentration of counterions confined in the inner domain. This result precludes the use of such a simple approach to determining the net interparticle force.

The fraction of counterions confined between the charged disks is estimated by integration of the ionic concentration profiles within the cylinder limited by the two parallel disks (inner ions). To better visualize the influence of confinement, it is compared with the fraction of counterions located within the two cylinders limited by one disk and the upper or lower boundary of the simulation cell (outer ions). The counterions located in the electrostatic well between the particles may be considered as adsorbed, defining the adsorbing capacity of the disks. This parameter is useful in order to quantify their potential use as an ionic exchanger or storing agent. As shown in Figure 3, this fraction varies as a function of the interparticle separation: more counterions are adsorbed when particles come close together because of the deeper overlap of their electrostatic wells in the inner domain.

Figure 4 further exhibits the heterogeneity of the ionic concentration profiles by displaying the longitudinal and radial variation of the ion local density. The shape and spatial extent of the ionic cloud are key factors which monitor the nematic organization[31,33] of anisotropic charged particles within diluted suspension. Figure 4 also sets to 40 Å the upper limit of the influence of border effects on the ionic distribution.

(B) Interparticle Interactions. We have calculated the net force exerted on each particle from thermalized ionic distributions (cf. eq 2). The results are shown in Figure 5 for disks neutralized by mono- and divalent counterions. The net force is divided by the cross section of the disk in order to be compared with the pressure calculated previously for infinite charged lamellae.[21−22] Because of the finite size of the particles, counterions are located on both sides, and the net contribution of the ion/disk longitudinal electrostatic and contact forces

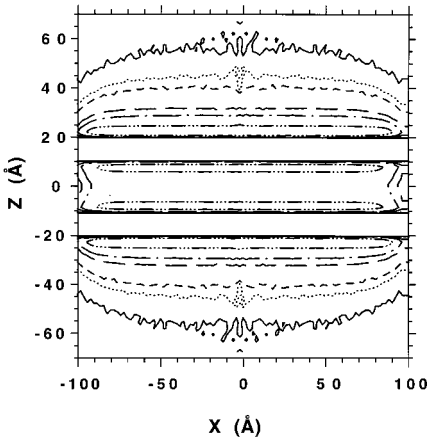

Figure 4. Radial section displaying contour plots of the reduced ionic densities in the vicinity of the two charged disks. The width of the plot is 200 Å, i.e, the diameter of the disks and the center/center separation between the disks is 30 Å. The contour plots are drawn for $c_i(\mathbf{r})/c_i^\circ$ = 3000 (—•••—), 1000 (—•—), 500 (— —), 100 (- -), 50 (...), and 10 (—).

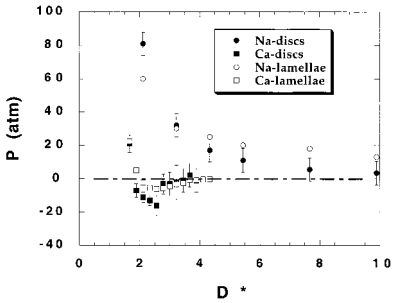

Figure 5. Pressure (atm) acting on charged disk and infinite lamellae as a function of the valency of the neutralizing counterion. For finite disks, the pressure is calculated from the net interparticular force divided by the disk cross section. The uncertainties in results reported for infinite lamellae are smaller than the size of the points.

cannot be predicted a priori. As an example, the net contact force exerted by the condensed counterions on each disk results from a balance between repulsive contribution from inner ions and attractive contribution from outer ions. However, because of the dissymmetry reported in Figure 2, one may conclude that there is a net repulsive ion/disk contact force.

The results shown in Figure 5 are in qualitative agreement with the data previously reported for infinite charged lamellae.[21−22] By contrast, the electrostatic and contact contributions differ totally (cf. Table 1). For infinite lamellae neutralized by mono- and divalent counterions, the net longitudinal pressure resulted from the balance between large electrostatic attraction and contact repulsion:

$$P = -\frac{\sigma^2}{2\,\epsilon_0\epsilon_r} + kT\,c_i(0) \qquad (4)$$

But for finite particles neutralized by monovalent counterions, the electrostatic contribution is always negligible (cf. Table 1), and the net longitudinal force results mainly from the repulsive contact force, because of the excess of condensed counterions in the inner domain. For charged disks neutralized by divalent counterions, the contact contribution to the longitudinal force is still repulsive, but the electrostatic attraction becomes significant and may overcome the contact repulsion, leading to attracto/repulsive behavior. This attraction is responsible for the flocculation reported for dilute suspensions of such colloidal anisotropic particles in the presence of divalent counterions.[37]

TABLE 1: Total Pressure (atm) and Its Contact Contribution for Particles Neutralized by Monovalent and Divalent Counterions

Monovalent Counterions				
	finite discs		infinite lamellae	
D^*	P_t	P_{cont}	P_t	P_{cont}
2.11	60 ± 7	61	81 ± 8	159
3.22	30 ± 7	38	32 ± 5	110
4.33	25 ± 6	25	17 ± 4	95
5.44	20 ± 6	19	11 ± 3	89
7.66	18 ± 6	14	6 ± 2	84
9.88	13 ± 6	11	3 ± 1	81
14.53	11 ± 6	9	1.7 ± 0.5	79.7
21.	6 ± 6	6	2.6 ± 0.5	80.6

Divalent Counterions				
	finite disks		infinite lamellae	
D^*	P_t	P_{cont}	P_t	P_{cont}
1.67	21 ± 5	66	22 ± 2	100
1.89	−7 ± 4	43	5 ± 1	83
2.11	−11 ± 3	30	−2 ± 1	76
2.33	−13 ± 3	22	−6 ± 1	72
2.56	−3 ± 6	15	−6 ± 1	72
2.78	−2 ± 10	16	−6 ± 1	72
3.00	−1 ± 7	15	−4.5 ± 0.5	74
3.22	2 ± 7	10	−3.2 ± 0.3	74.8
3.44	−1 ± 7	12	−2.5 ± 0.3	75.5
	3.67		−0.6 ± 0.1	77.4
	3.89		−0.6 ± 0.1	77.4
4.11	−0.5± 0.1		77.5	
4.33	−0.3± 0.1		77.7	

Finally, at large separation, the contact force between two finite disks becomes negligible, since the local ionic concentration is the same at both sides of the disks. Note that totally different behavior is reported for infinite charged lamellae.

4. Conclusion

Ionic distributions around two finite charged disks are calculated by (N,V,T) Monte Carlo simulations in the framework of the primitive model. While the net force agrees qualitatively well with the results obtained previously for infinite charged lamellae, the electrostatic and contact contributions differ totally. We further test the validity of the Weak Overlap Approximation as a functional approach able to describe a large collection of anisotropic charged particles as a One Component Plasma.

Acknowledgment. We cordially thank Drs J.L. Raimbault and H.van Damme for their interest in the progress of this work. Monte Carlo simulations where performed locally on workstations purchased thank to grants from Région Centre (France).

References and Notes

(1) Morawetz, H. *Polyelectrolyte Solutions*; Academic Press: New York, 1961; Chapter 5.
(2) Rogers, F. J. *J. Chem. Phys.* **1980**, *7*, 6272.
(3) Van Megen, W.; Snook, I. *J. Chem. Phys.* **1980**, *73*, 4656.
(4) Anderson, J. L. *J. Coll. Interface Sci.* **1985**, *105*, 45.
(5) Guldbrand, L.; Jönsson, B.; Wennerström, H.; Linse, P. *J. Chem. Phys.* **1984**, *80*, 2221.
(6) Overbeek, J. Th. G. *J. Chem. Phys.* **1987**, *87*, 4406.
(7) Fair, M. C.; Anderson, J. L. *J. Coll. Interface Sci.* **1989**, *127*, 388.
(8) Kjellander, R.; Marcelja, S.; Pashley, R. M.; Quirk, J. P. *J. Phys. Chem.* **1988**, *92*, 6489.
(9) Valleau, J. P.; Ivkov, R.; Torrie, G. M. *J. Chem. Phys.* **1991**, *95*, 520.
(10) Bratko, D.; Henderson, D. *Electrochim. Acta* **1991**, *36*, 1761.
(11) Löwen, H.; Hansen, J. P.; Roux, J. N. *Phys. Rev. A: At., Mol., Opt. Phys.* **1991**, *44*, 1169.

(12) Löwen, H.; Madden, P. A.; Hansen, J. P. *Phys. Rev. Lett.* **1992**, *68*, 1081.
(13) Dubois, M.; Zemb, Th.; Belloni, L.; Delville, A.; Levitz, P.; Setton, R. *J. Chem. Phys.* **1992**, *96*, 2278.
(14) Kjellander, R. Åkesson, T.; Jönsson, B.; Marcelja, S. *J. Chem. Phys.* **1992**, *97*, 1424.
(15) Löwen, H.; Hansen, J. P.; Madden, P. A. *J. Chem. Phys.* **1993**, *98*, 3275.
(16) Chang, F. R. Ch.; Sposito, G. *J. Coll. Interface Sci.* **1994**, *163*, 19.
(17) Delville, A. *Langmuir* **1994**, *10*, 395.
(18) Chang, F. R. Ch.; Sposito, G. *J. Coll. Interface Sci.* **1996**, *178*, 555.
(19) Linse, P.; Jönsson, B. *J. Chem. Phys.* **1983**, *78*, 3167.
(20) Hsu, J. P.; Tseng, M. T. *Langmuir* **1997**, *13*, 1810.
(21) Delville, A.; Pellenq, R. J. M.; Caillol, J. M. *J. Chem. Phys.* **1997**, *106*, 7275.
(22) Pellenq, R. J. M.; Caillol, J. M.; Delville, A. *J. Phys. Chem. B* **1997**, *101*, 8584.
(23) Delville, A.; Gasmi, N.; Pellenq, R. J. M.; Caillol, J. M.; Van Damme, H. *Langmuir* **1998**, *14*, 5077.
(24) Allahyarov, E.; D'Amico, I.; Löwen, H. *Phys. Rev. Lett.* **1998**, *81*, 1334.
(25) McCormack, D.; Carnie, S. L.; Chan, D. Y. C. *J. Colloid. Interface Sci.* **1995**, *169*, 177.
(26) Gabriel, J. C. P.; Sanchez, C.; Davidson, P. *J. Phys. Chem.* **1996**, *100*, 11139.
(27) Mourchid, A.; Lécolier, E.; Van Damme, H.; Levitz, P. *Langmuir* **1998**, *14*, 4718.
(28) Pignon, F.; Magnin, A.; Piau, J. M.; Cabane, B.; Lindner, P.; Diat, O. *Phys. Rev. E: Stat. Phys., Plasmas, Fluids, Relat. Interdiscip. Top.* **1997**, *56*, 3281.
(29) Kroon, M.; Vos, W. L.; Wegdam, G. H. *Phys. Rev. E: Stat. Phys., Plasmas, Fluids, Relat. Interdiscip. Top.* **1998**, *57*, 1962.
(30) van der Kooij, F. M.; Lekkerkerker, H. N. W. *J. Phys. Chem. B* **1998**, *102*, 7829.
(31) Mourchid, A.; Delville, A.; Lambard, J.; Lécolier, E.; Levitz, P. *Langmuir* **1995**, *11*, 1942.
(32) Dijkstra, M.; Hansen, J. P.; Madden, P. A. *Phys. Rev. E: Stat. Phys., Plasmas, Fluids, Relat. Interdiscip. Top.* **1997**, *55*, 3044.
(33) Forsyth, P. A.; Marcelja, S.; Mitchell, D. J.; Ninham, B. *Adv. Colloid Interface Sci.* **1978**, *9*, 37.
(34) Heyes, D. M. *Phys. Rev. B: Condens. Matter* **1994**, *49*, 755.
(35) Zhang, L.; White, H. S.; Davis, H. T. *Mol. Simul.* **1992**, *9*, 247.
(36) Sogami, I. S.; Shinohara, T.; Smalley, M. V. *Mol. Phys.* **1992**, *76*, 1.
(37) Mourchid, A.; Levitz, P. *Phys. Rev. E: Stat. Phys., Plasmas, Fluids, Relat. Interdiscip. Top.* **1998**, *57*, R4887.
(38) Thompson, D. W.; Butterworth, J. T. *J. Coll. Interface Sci.* **1992**, *151*, 236.
(39) van Olphen, H. *An Introduction to Clay Colloid Chemistry*; Interscience Publishers: New York, 1963; Chapter 7.
(40) Hummer, G. *Chem. Phys. Lett.* **1995**, *235*, 297.